Supporting Information for

Molecular engineering of a secreted, highly homogenous and neurotoxic Aβ dimer by Andreas Müller-Schiffmann et al.

1. Computational simulations of the Aβ-dimer structure

Rationale for the computational setup:

In contrast to Aβ-fibrils, which adopt a well-defined U-shaped topology (*1, 2*), Aβ dimers exhibit a much larger conformational flexibility. In this context, computational studies detected that the U-shaped fold present in the fibril is rather unstable in the Aβ-dimer and the dimer preferentially adopts alternative conformations that allow additional stabilization by the formation of a larger hydrophobic core or by novel β-strands (*3, 4*) (Fig. 1c).

These additional modes of stabilization render the respective Aβ-species remarkably stable (*3, 4*) and the significant structural deviation from the fibril-like topology suggests that these alternative conformations are rather elongation-incompetent (*3*). The presence of such elongation-incompetent Aβ-dimer species is also supported by the experimental observation that Aβ dimers act only as poor seeds for fibril formation (*5*) and might also explain the high dimer toxicity.

In our computational investigations we focused on the question whether the mutant, disulfide-bonded Aβ dimers exhibit the same structural properties as the wildtype Aβ dimers. In this context, it was of particular interest to assess the relative stabilities of the U-shaped fibril-like dimer conformation compared to alternative elongation-incompetent conformations.

Structural properties of the wiltype and mutant Aβ-dimers:

The root mean square deviation (RMSD) as a function of the simulation time (Fig. S1a) showed that all four systems studied deviated significantly from the U-shaped starting topology. The RMSDs of 10-15 Å that we detected were significantly larger than the values of 1-3 Å generally found in globular proteins. This indicated that the U-shaped topology present in the fibril was only marginally stable both in wildtype and mutant Aβ(1-42) simulated and that elongation-incompetent conformations formed instead. For wildtype Aβ dimers, this observation was in line with the experimental observation that wildtype Aβ dimers act as poor seeds for fibril formation compared to trimers and tetramers (*5*), as well as with previous theoretical studies (*3, 4*). While the degree of deviation from the U-shaped starting structure was similar for wildtype, S8C and M35C mutants, larger deviations were observed for the S26C mutant suggesting that this mutant adopted a distinct and different structure (Fig. S1b).

Analysis of the most populated conformations sampled during the MD simulations revealed that wildtype Aβ and two of the mutants (Aβ S8C, M35C) underwent major changes in their C-terminus and preferentially adopted a conformation exhibiting an additional antiparallel β-sheet in one of the subunits (Fig. 2, Fig. S2). This conformational rearrangement allows efficient shielding of hydrophobic residues from the solvent. The structure of this hydrophobic core is shown in detail in Fig. 2 and the solvent accessibility of the respective residues is given in the Supplementary Table S1.

Table S1 shows that wildtype and S8C mutant adopt a conformation, which allows a highly efficient shielding of residues L17, F19, and A21 of chain B. In particular, F19 is almost completely inaccessible to the solvent. A shielding of the phenylalanines is also detected but less pronounced on the M35C mutant. Generally, table S1 shows that in the wildtype and S8C / M35C mutants four to five of the six residues investigated are highly buried from solvent (bold values in Table S1). Interestingly, such a shielding is not observed for the S26C mutant. In this mutant, which adopts a rather planar arrangement, only two of the six residues are significantly buried from the solvent (Fig. 2, Table S1).

In summary, one can conclude that all Aβ-dimers studied preferentially adopt elongation-incompetent conformations, and that the S26C-dimer exhibits distinct structural properties from that of the other dimers.

2. Supplementary Table 1

Solvent accessible surface area (SASA) of the Central Hydrophobic Core residues L17, F19, and A21 of wildtype and mutant Aβ-dimers. Values were calculated individually for chain A and B of the most representative cluster structure. All values are given in $Å^2$. Highly buried residues, which expose ≤ 25% of their total surface area to the solvent, are given in bold and marked by an asterisk.

System	Chain	Leu17	Phe19	Ala21
WT	A	81	132	**39***
	B	**22***	**0***	**17***
S8C	A	**24***	**40***	71
	B	**26***	**2***	**2***
S26C	A	**24***	87	**11***
	B	54	69	49
M35C	A	**28***	**28***	**17***
	B	69	**47***	**6***

3. Supplementary Figures

Supplementary Figure S1.

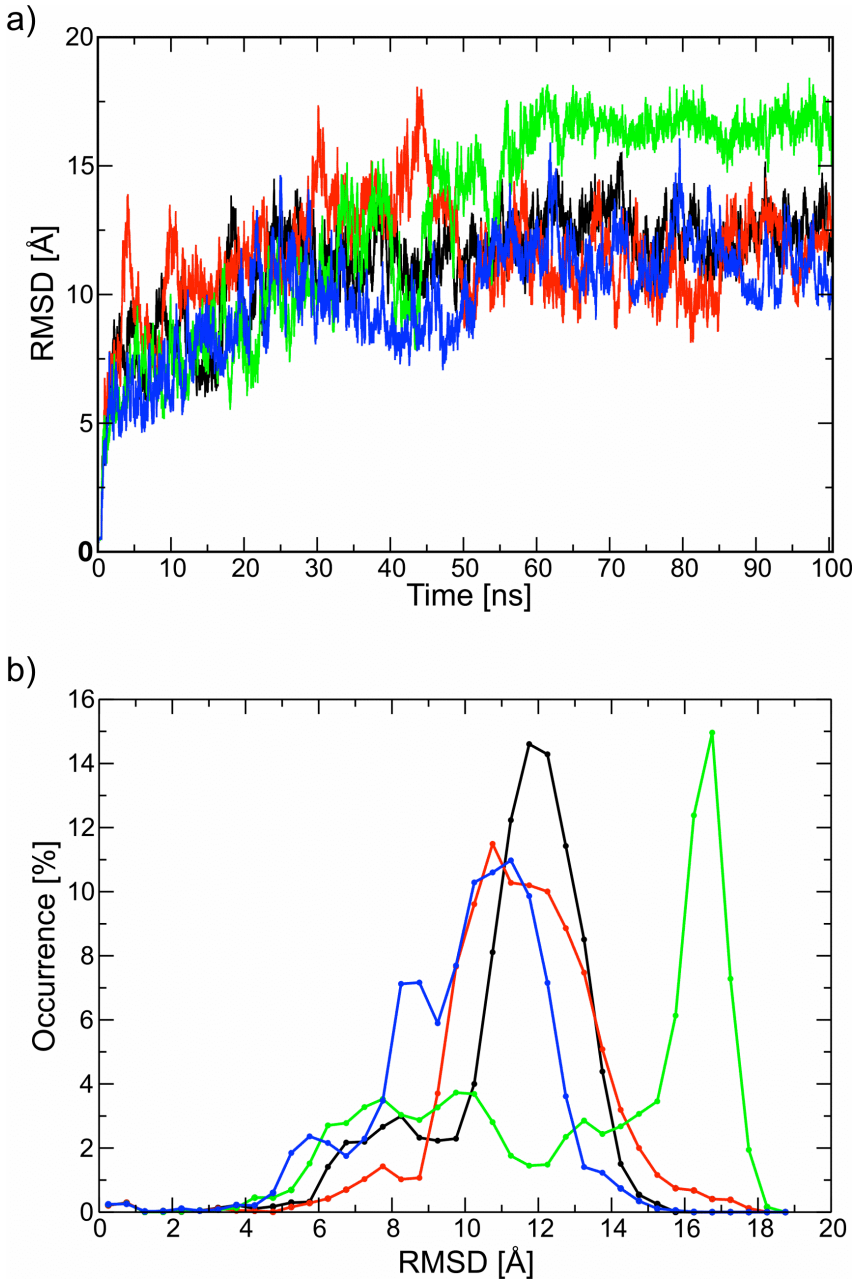

Plot of the conformational stability of wildtype and disulfide-bonded mutant Aβ-dimers in the course of the 100-ns molecular dynamics simulations. a) The high RMSD values indicate that the U-shaped topology of the starting structure is only marginally stable in all systems studied and that the largest deviations are observed for the S26C-mutant (green curve). b) Relative population (occurrence) of the different Aβ-species sampled over the MD simulation with respect to their similarity to the starting structure. Note that wildtype (black),

S8C (red), and M35C (blue) exhibit similar features, while S26C (green) shows distinct properties.

Supplementary Figure S2

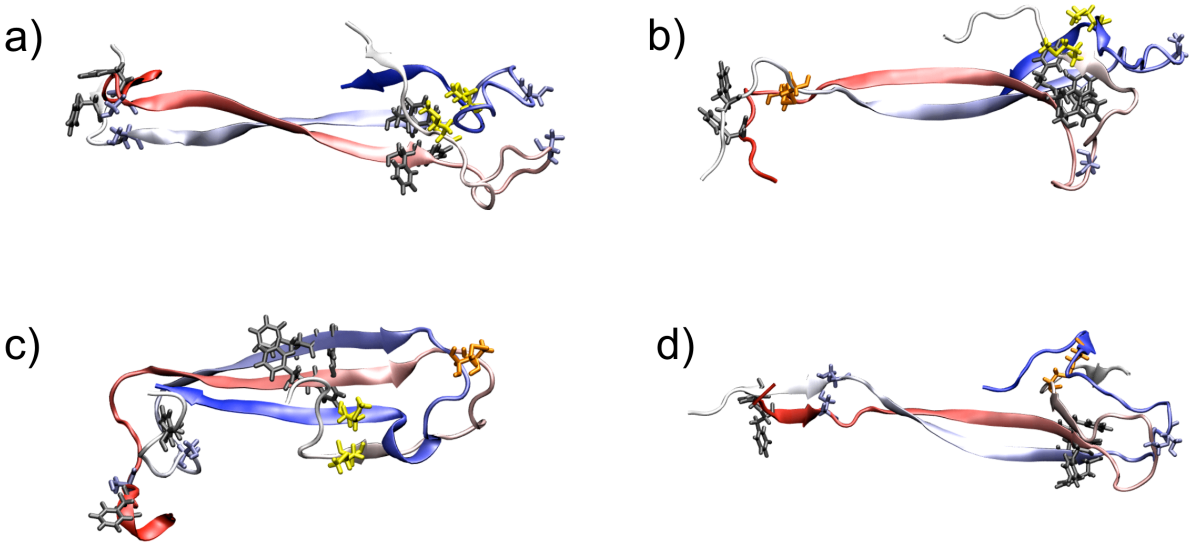

Molecular structure of the most populated Aβ-conformation for wildtype (a), S8C (b), S26C (c), and M35C (d) that was present in the respective molecular dynamics simulations. The Aβ S8C and M35C mutants exhibit similar structural properties than the wildtype and display an intramolecular antiparallel β-sheet in chain that allows shielding of the hydrophobic core from the solvent. In contrast, S26C shows a different β-sheet arrangement. The two chains of the Aβ-dimer are shown as red and blue ribbon. Cysteines, methionines, and aromatic residues are shown as orange, yellow, and grey sticks, respectively.

Supplementary Figure S3.

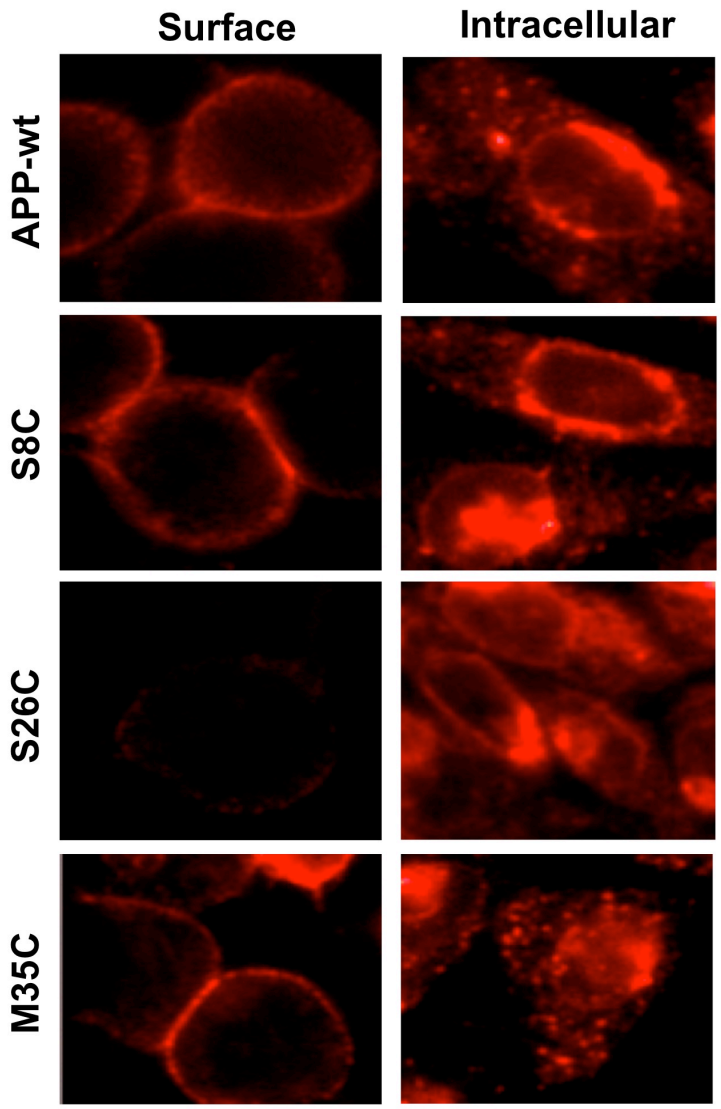

Intracellular and surface staining of CHO cells overexpressing wt or mutant APP. Cells were treated with γ-secretase inhibitor LY411575 (Eli Lilly, Indianapolis, IN) to enable surface staining using the 4G8 antibody (Signet, Dedham, MA) and a mouse IgG specific Alexa flour 594 antibody (Thermo Scientific, Bonn, Germany). While intracellular APP concentrations were comparable, CHO cells expressing APP S26C showed a strongly reduced presence of APP at the surface, indicating a reduced trafficking of APP- AβS26C to the cell surface.

Intracellular and cell surface staining. Cells were grown on glass cover slips in 24 well plates to confluency. To allow detection of surface APP, cells were incubated with 10 nM of

γ-secretase inhibitor LY411575 (Eli Lily, Indianapolis, IN). For cell surface staining cells were rinsed in PBS and incubated 60 min with 4G8 diluted 1:200 in PBS/ 2% BSA. After washing three times with PBS cells were fixed in PBS/4% paraformaldehyde for 10 min on ice and washed again with PBS before incubation with Alexa-Fluor 594 conjugated goat anti-mouse IgG diluted 1:200 in PBS/ 2% BSA for 30 min at RT. After washing with PBS cells were analyzed by fluorescence microscopy. For intracellular staining cells were first fixed and then permeabilized with 0.5% saponine at RT for 30 min prior antibody incubation.

Supplementary Figure S4.

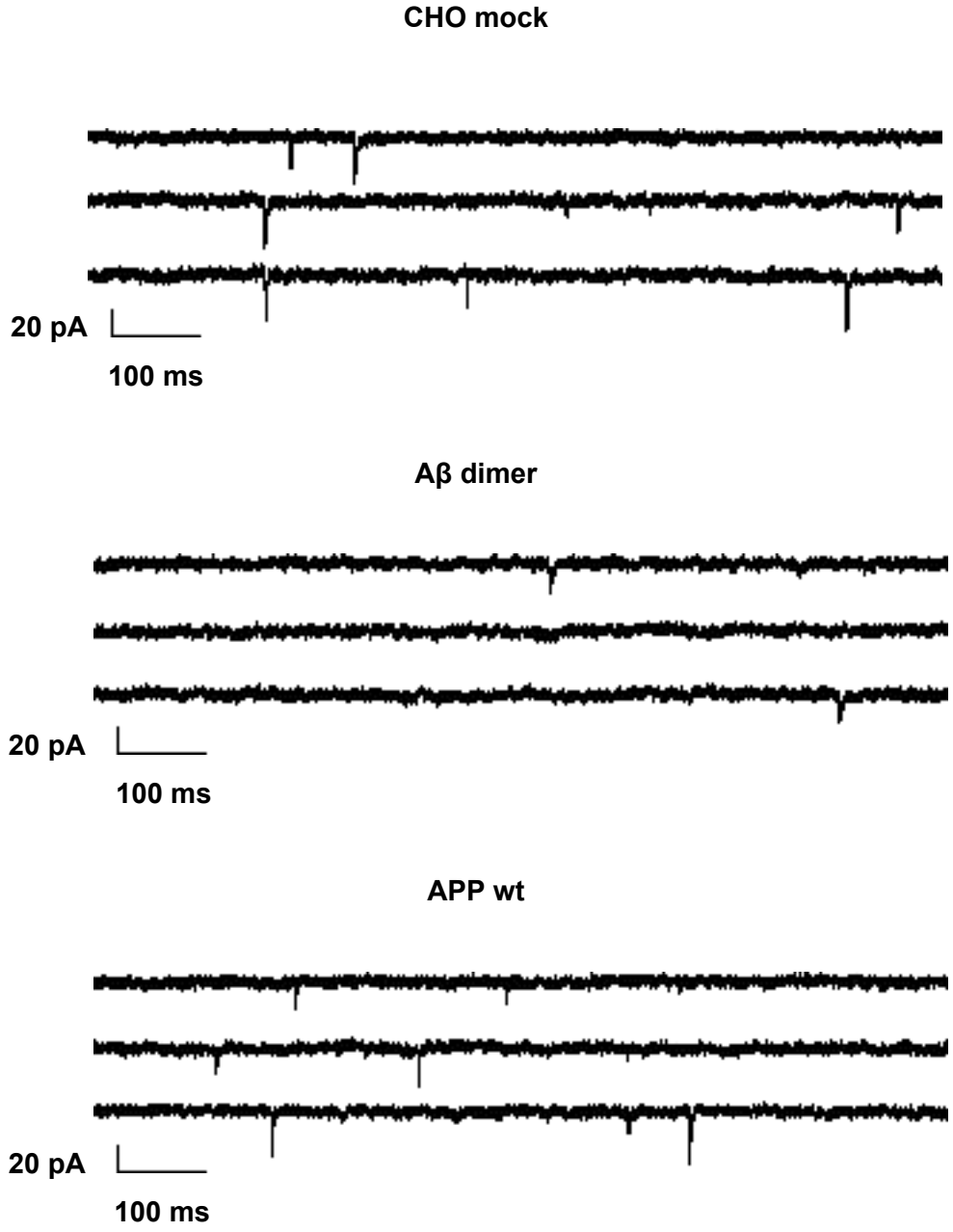

AβS8C dimer decreases mEPSC frequency and amplitude in cultured cortical neurons. Example traces of AMPA receptor mediated miniature EPSCs. mEPSC frequency and amplitude were significantly decreased in cortical neurons incubated for 4 days with supernatant containing AβS8C dimers (*Aβ dimer*) when compared with neurons incubated with CHO mock (*CHO mock*) or with the supernatant that was produced by CHO cells transfected with APP wt (*APP wt*).

References

1. Petkova, A. T., Leapman, R. D., Guo, Z., Yau, W. M., Mattson, M. P., and Tycko, R. (2005) Self-propagating, molecular-level polymorphism in Alzheimer's beta-amyloid fibrils, *Science 307*, 262-265.
2. Lührs, T., Ritter, C., Adrian, M., Riek-Loher, D., Bohrmann, B., Dobeli, H., Schubert, D., and Riek, R. (2005) 3D structure of Alzheimer's amyloid-beta(1-42) fibrils, *Proc. Natl. Acad. Sci. U S A 102*, 17342-17347.
3. Horn, A. H., and Sticht, H. (2010) Amyloid-beta42 oligomer structures from fibrils: a systematic molecular dynamics study, *J. Phys. Chem. B 114*, 2219-2226.
4. Huet, A., and Derreumaux, P. (2006) Impact of the mutation A21G (Flemish variant) on Alzheimer's beta-amyloid dimers by molecular dynamics simulations, *Biophys. J. 91*, 3829-3840.
5. Ono, K., Condron, M. M., and Teplow, D. B. (2009) Structure-neurotoxicity relationships of amyloid beta-protein oligomers, *Proc. Natl. Acad. Sci. U S A 106*, 14745-14750.